Supporting information

Kinetics of Low-Pressure, Low-Temperature Graphene Growth: Towards Single-Layer, Single-Crystalline Structure

Hamid Mehdipour and **Kostya (Ken) Ostrikov***

Plasma Nanoscience Centre Australia (PNCA), CSIRO Materials Science and Engineering,

P.O. Box 218, Lindfield, New South Wales 2070, Australia, and Plasma Nanoscience @ Complex Systems, School of Physics, University of Sydney, New South Wales 2006, Australia

*Address correspondence to *kostya.ostrikov@csiro.au*

This **Supporting Information** file includes:

Model equations, discussions, explanations, and figures S1 to **S5**
References RS1 to **RS30**

Numerical model and main assumptions

Here, the model of the neutral-gas interactions on a metal surface exposed to a neutral gas of C_2H_4/H_2+CH_4 mixtures is presented. Due to direct adsorption of hydrocarbon molecules and hydrogen atoms/molecules on the bare metal surface they undergo thermal/hydrogen-induced dissociation (TD/HID) and carbon atoms (building units (BUs)) are generated as a result (see Figure 1 in the main text).[RS1,RS2] Because of the extremely low solubility of carbon atoms in Cu[RS3] and Ru/Ir[RS4] (in the temperature range considered here) the carbon diffusion into the metal bulk and then segregation into the surface are very unlikely to happen. So, all the BU creation/loss processes as well as graphene nucleation and growth processes take place on the top surface of the metal substrate. The carbon atoms (BUs) are created via TD/HID of C_2H_4/CH_4 molecules.[RS4-RS6] The BUs diffuse on the metal surface and agglomerate forming the 5 C atom clusters as intermediate C structures during the graphene nucleation.[RS6] The clusters formed diffuse and collide with each other and nucleate graphene nuclei. The most stable carbon nuclei predicted experimentally and theoretically to form at the initial stage of graphene nucleation on the transition-metal substrates contain 7 honeycomb units.[RS7,RS8] Therefore, here, we assume that 6 carbon clusters contribute to the graphene nucleus formation, which is known as the early stage in graphene growth. This assumption made since previous numerical work[RS9] introduced this nucleus configuration not only as the optimum nucleus structure that enables the numerical solution to reproduce the main features of the experimental data,[RS4] but also it has a similar number of BUs to stable graphene structures observed by Scanning Tunneling Microscopy[RS7] and predicted by DFT calculations.[RS8,RS10] After the graphene nuclei are formed, they grow

together or diffuse and stitch to each other producing larger graphene islands. The latter process is called Smoluchowski ripening which strongly depends on the initial graphene nucleus density (or initial distance between graphene islands) as well as the surface temperature.[RS11] The BU production on the metal surface becomes less effective with increasing the graphene surface coverage. This is because access of precursor hydrocarbon molecules to bare metal surface is reduced when the graphene domains cover the surface. This in turn leads to less effective thermal/hydrogen-induced decomposition of the precursor molecules.

The set of equations used to describe the graphene nucleation and growth includes

$$\frac{dn_{\mathrm{H}}}{dt} = J_{\mathrm{H}}\left(1-\theta_G\right) - n_{\mathrm{H}} n_{\mathrm{CH_4}} \nu \exp\left(-E_{\mathrm{sdH}}/kT\right) - n_{\mathrm{H}}^2 \nu \exp\left(-E_{\mathrm{sdH}}/kT\right) - n_{\mathrm{H}} \nu \exp\left(-E_{\mathrm{desH}}/kT\right) \quad \text{(S-1)}$$

$$\frac{dn_{\mathrm{CH_4}}}{dt} = J_{\mathrm{CH_4}}\left(1-\theta_G\right) - n_{\mathrm{H}} n_{\mathrm{CH_4}} \nu \exp\left(-E_{\mathrm{sdH}}/kT\right) - n_{\mathrm{CH_4}} \nu \exp\left(-E_{\mathrm{desCH}}/kT\right) \quad \text{(S-2)}$$

$$\frac{dn_{\mathrm{CH_j}}}{dt} = n_{\mathrm{H}}\left(n_{\mathrm{CH}_{j+1}} - n_{\mathrm{CH}_j}\right)\nu \exp\left(-E_{\mathrm{sdH}}/kT\right) \quad , \quad \text{j=1,2, and 3} \quad \text{(S-3)}$$

$$\frac{dn_{\mathrm{C_2H_4}}}{dt} = J_{\mathrm{C_2H_4}}\left(1-\theta_G\right) - n_{\mathrm{C_2H_4}} \nu \exp\left(-E_{\mathrm{tdCH}}/kT\right) - n_{\mathrm{C_2H_4}} \nu \exp\left(-E_{\mathrm{desCH}}/kT\right) \quad \text{(S-4)}$$

$$\frac{dn_{\mathrm{C}}}{dt} = J_C^+ - J_C^- \quad \text{(S-5)}$$

$$\frac{dn_{\mathrm{CL}}}{dt} = n_C^{\mathrm{m}} \nu \exp\left(-E_{\mathrm{sdC}}/kT\right) - n_{\mathrm{CL}} \nu \exp\left(-E_{\mathrm{tdCL}}/kT\right) - p n_{\mathrm{CL}}^{\mathrm{p}} \nu \exp\left(-E_{\mathrm{sdCL}}/kT\right) -$$

$$n_{\mathrm{CL}} n_{\mathrm{IS}} \nu \exp\left(-E_{\mathrm{sdCL}}/kT\right) \quad \text{(S-6)}$$

$$\frac{dn_{\mathrm{IS}}}{dt} = n_{\mathrm{CL}}^{p} \nu \exp\left(-E_{\mathrm{sdCL}}/kT\right) - 2n_{\mathrm{IS}} \frac{d\theta_{\mathrm{G}}}{dt} - 8\nu \exp\left(-E_{\mathrm{sdIS}}/kT\right) \theta_{\mathrm{G}}^{\alpha} \left(1-\theta_{\mathrm{G}}^{1/2}\right)^{-2} n_{\mathrm{IS}}^{2-\alpha} \quad \text{(S-7)}$$

$$\frac{d\theta_{\mathrm{G}}}{dt} = (m \times p) n_{C}^{\mathrm{m}} \nu \exp\left(-E_{\mathrm{sdCL}}/kT\right) + n_{\mathrm{CL}} n_{\mathrm{IS}} \nu \exp\left(-\left(E_{\mathrm{sdCL}} + E_{\mathrm{incCL}}\right)/kT\right) +$$

$$n_{\mathrm{C}} n_{\mathrm{IS}} \nu \exp\left(-\left(E_{\mathrm{sdC}} + E_{\mathrm{incC}}\right)/kT\right) \quad \text{(S-8)}$$

for hydrogen atoms (H), CH_4 molecules, hydrocarbon radicals (CH, CH_2, and CH_3), C_2H_4 molecules, carbon atoms, 5-C clusters, graphene nuclei/islands, and surface coverage by graphene, respectively. The first term in Eq. (S-1) describes the hydrogen atom adsorption (on the bare Cu surface), whereas the second, third, and fourth terms describe hydrogen atom loss through hydrogen-induced dehydrogenation (HID, with the energy barrier E_{sdH}), hydrogen atom recombination, and hydrogen desorption, respectively. The first term in Eq. (S-2) describes the reduction in the adsorption flux of hydrocarbons (due to the graphene covering the bare metal surface), while the second and third terms account for loss of CH_4 molecules due to HID and thermal desorption (with energy barrier E_{desCH}) from the Cu metal surface. Equation (S-3) describes the creation (of radicals with fewer hydrogen atoms) and loss reactions involved in HID. The first term in Eq. (S-4) describes the reduction in the C_2H_4 adsorption flux to the Ru/Ir surface (due to the graphene covering the bare metal surface), while the second and third terms account for loss of C_2H_4 molecules due to TD and thermal desorption (with energy barrier E_{desCH}) from the metal surface. In above Eqs., $J_{\alpha} = P_{\alpha} v_{\mathrm{th},\alpha} / (4T)$ and n_{α}

denote the flux of species α and its concentration on the surface, respectively, where P_α is the pressure of α gas and $v_{\mathrm{th},\alpha}$ is thermal speed of α species. Here, $\alpha = \mathrm{H}, \text{and } \mathrm{CH_4/C_2H_4}$ stand for hydrogen atoms and hydrocarbon molecules, respectively.

In Eq. (S-5)

$$J_C^+ = n_{\mathrm{C_2H_4}} \nu \exp\left(-E_{\mathrm{tdCH}}/kT\right)\left[n_{\mathrm{H}} n_{\mathrm{CH}} \nu \exp\left(-E_{\mathrm{sdH}}/kT\right)\right] + n_{\mathrm{CL}} \nu \exp\left(-E_{\mathrm{tdCL}}/kT\right) + (m \times p) n_{\mathrm{IS}} \nu \exp\left(-E_{\mathrm{tdIS}}/kT\right)$$

describes creation of carbon atoms due to TD [HID], dissociation of carbon clusters (with energy barrier E_{tdCL}) and graphene nucleus (with energy barrier E_{tdIS}), whereas

$$J_C^- = n_{\mathrm{C}} \nu \exp\left(-E_{\mathrm{evC}}/kT\right) + n_{\mathrm{C}}\left(J_{\mathrm{H}} + n_{\mathrm{H}} \nu \exp\left(-E_{\mathrm{sdH}}/kT\right)\right) + m n_C^{\mathrm{m}} \nu \exp\left(-E_{\mathrm{sdC}}/kT\right) + n_{\mathrm{C}} n_{\mathrm{IS}} \nu \exp\left(-\left(E_{\mathrm{sdC}} + E_{\mathrm{incC}}\right)/kT\right)$$

describes loss of carbon atoms due to evaporation (EV, with energy barrier E_{evC}), hydrogen-induced etching (HIE), formation of m-C clusters ($m = 5$), and carbon atom incorporation into the graphene network (with energy barrier E_{incC}). Here, n_{C}, n_{CL}, and n_{IS} are the surface concentrations of carbon atoms, 5-C clusters, and graphene nuclei, respectively. In Eq. (S-6), except for the first term which describes the creation of 5-C atom clusters, the second, third, and fourth terms account for the cluster loss due to dissociation of C clusters, formation of graphene nuclei (from $p = 6$ clusters), cluster incorporation into the graphene network, respectively. The first, second, and third terms in Eq. (S-7) account for the formation of graphene nuclei, growth of graphene islands, and Smoluchowski

ripening of graphene islands,[RS11] respectively. $\alpha(\approx 1.5)$ in the ripening term denotes the dependence of the island surface diffusion on the average size of the graphene islands.[RS11] Finally, the Eq. (S-8) describes the total graphene surface coverage (θ_{G}) due to formation of graphene nuclei (first term) as well as incorporations of the carbon atoms and clusters (second and third terms) into the graphene network. In Eqs. (S-1)-(S-8), ν is the thermal vibrational frequency and the lattice constant a_0 has been set to unity, *i.e.*, $a_0 = 1.0$.

The above equations are solved numerically and the surface concentrations of key species (*e. g.*, C atoms, hydrogen atoms, *etc.*) as well as the graphene growth parameters (*e. g.*, graphene island density, graphene surface coverage) are obtained as functions of time. In the present work, the hydrogen/hydrocarbon pressure $P_{\mathrm{H}} / P_{\mathrm{CH_4/C_2H_4}}$ and substrate temperature T are used as input parameters in the computations.

Very-low-pressure CVD of graphene on Ru: effect of temperature

The surface concentration of C atoms n_{C} as a function of time t has been plotted at different temperatures in Figure S1. It is clearly seen that graphene nucleates only when the catalyst temperature has been raised above the threshold value ($T = 570\,\mathrm{K}$). This clearly demonstrates the minimum-temperature requirement for the graphene nucleation, which was evidenced by experimental observation of no graphene nucleation at very low temperatures even with a constant supply of a precursor gas.[RS12] The nucleation time t_{n} decreases with increasing the temperature in the low-temperature range ($550 < T < 800\,\mathrm{K}$), whereas it increases with T in the high-temperature range. This can be understood by noting that with increasing the temperature, TD of the hydrocarbon molecules becomes more effective, so more C atoms are generated and contribute into C-cluster formation. Hence, more clusters are produced within a shorter time, so the graphene nucleation happens faster at higher temperatures. However, with increasing T in the

high-temperature range, despite the enhanced creation of carbon atoms, the hydrocarbon desorption and C evaporation (EV) become more effective as well. In this case, the C loss dominates over C production on the bare metal surface, and hence, the graphene nucleation takes place within shorter times. Also, the C concentration required for graphene nucleation ($n_{\mathrm{C}}^{\mathrm{nuc}}$) and C concentration at equilibrium stage ($n_{\mathrm{C}}^{\mathrm{eq}}$) show different trends with increasing T in the low- and high-temperature ranges (see Figure S2). It is seen in Figure S2 that the numerically-calculated concentrations, $n_{\mathrm{C}}^{\mathrm{nuc}}$ and $n_{\mathrm{C}}^{\mathrm{eq}}$, first increase with T, whereas they decrease with a further increase in T. The computed changes in $n_{\mathrm{C}}^{\mathrm{nuc}}$ and $n_{\mathrm{C}}^{\mathrm{eq}}$ (with the increase of the catalyst temperature) are similar in trend to the changes in the equivalent concentrations measured in the CVD experiment using ethylene as the precursor gas.[RS4] This good agreement between the numerical and the experimental results further confirms the validity of the numerical model developed.

Low-pressure CVD of graphene on Cu: effects of hydrogen/hydrocarbon pressure and temperature

It was mentioned (in the main body of the main text) that hydrogen atoms have dual role in the nucleation and growth of graphene on Cu when methane (CH4) gas is used as the precursor gas.[RS5] This is shown in Figure S3, where the C concentration required for nucleation of C nuclei ($n_{\mathrm{C}}^{\mathrm{nuc}}$) is plotted as a function of hydrogen gas pressure (P_{H}). Hydrogen atoms adsorbed on the surface dehydrogenate the hydrocarbon molecules/radicals leading to production of building units (C atoms) required for graphene nucleation. The C atom creation is enhanced with increasing P_{H} as a result of a higher hydrogen flux to the bare metal surface which in turn results in more effective HID. However, further increasing in the hydrogen gas pressure leads to an effective hydrogen etching of the C atoms as well as hydrocarbon radicals from the substrate surface, which in turn leads to presence of smaller number of C atoms on the surface. Thus, $n_{\mathrm{C}}^{\mathrm{nuc}}$ decreases with further

increasing the hydrogen gas pressure (see Figure S3).

As was mentioned in the main text, with decreasing the bare surface area (due to increasing the graphene surface coverage) the adsorption of precursor molecules becomes less effective, which in turn less BUs are produced (on the surface) and then attach to the graphene (islands). Therefore, a decrease of the graphene growth rate is likely to happen with increasing the surface coverage (θ_G). This expected trend is obtained numerically and plotted in Figure S4, where functionality of graphene growth rate R_G on θ_G has been shown for different hydrocarbon gas pressures (Figure S4a) and catalyst temperatures (Figure S4b). R_G increases with increasing the hydrocarbon gas pressure (see Figure S4a) as a result of more intense fluxes of CH_4 molecules to the Cu catalyst surface which is followed by more effective dehydrogenation of the adsorbed molecules. This is in good agreement with the experimental results of Li *et al.*[RS13] More importantly, the computed trend of R_G (with increase of θ_G) is as same as the observed trend of change in graphene growth rate as the graphene monolayer covers the Cu surface in CVD experiment.[RS13]

Changes in the graphene growth parameters with increasing Cu catalyst temperature T are non-monotonic and show opposite trends in low- and high-temperature ranges under low-pressure CVD conditions (see Figure S4b and Figure S5). The first increase of graphene growth with increasing T can be attributed to more effective HID at high T. With a further increase in T, the hydrogen etching of carbon atoms (due to hydrogen atom-C monomer reactions, reaction (11) in Table 1 in the main text) prevails over the HID of the hydrocarbon molecules (CH_4). In this case, the BU surface concentration decreases, which leads to a lower graphene growth rate (see Figure S4b). As a result, the total graphene surface coverage decreases at a much higher catalyst temperatures, especially when the hydrogen gas pressure is so high (see Figure S5). These numerical results are consistence with reported minimum-temperature requirement for an effective etching of the monolayer graphene in the CVD experiment,[RS5] which indicates the important role of temperature in the effective

hydrogen etching of graphene layers and producing single-layer graphene.

Dehydrogenation of hydrocarbon molecules on a Cu surface: a discussion

Here we discuss possible channels of dehydrogenation (decomposition) of hydrocarbon (especially methane) molecules on a Cu catalyst surface. Direct decomposition of methane (CH_4) molecules on a Cu surface is energetically much less favourable compared to other metals.[RS14] Indeed, the activation energy of this process is very large, almost four times larger compared to a Ni surface.[RS15] Therefore, thermal decomposition of CH_4 is less likely to happen or, at least is much less effective compared to other cases. Moreover, the rate of C production from thermal decomposition of hydrocarbon molecules (in general, not only CH_4 molecules) is much lower on a Cu surface than on a Ni surface.[RS16] More importantly, La Cava *et al.* reported that no C deposition was detected at low temperatures when the hydrogen gas was not supplied.[RS16] These arguments evidence the less important role of the thermal decomposition in the production of C atoms that are required for the graphene nucleation and growth on the surface of a Cu substrate commonly used in graphene synthesis experiments.

However, other catalyst agents (such as hydrogen or oxygen atoms) can react with CH_4 molecules on the Cu (and other metal) surface leading to hydrogen abstraction (and eventually C production) from the CH_4 molecules.[RS2,RS15,RS16,RS17] This was evidenced experimentally by addition of hydrogen (oxygen) gas to the hydrocarbon gas (CH_4, during the growth step) and increasing the hydrogen partial pressure, which led to the initiation of graphene nucleation or an increase of the C deposition rate at all temperatures (on the Cu foil surface).[RS5,RS15,RS16] As mentioned above, C deposition experiment by La Cava *et al.* showed that no carbon material was found on the catalyst surface without addition of hydrogen gas at temperatures below 873 K.[RS16] Also, hydrogen annealing of the Cu catalyst foil/film leads to more effective enrichment of the catalyst surface with hydrogen atoms. These atoms then react with CH_4 molecules during the growth process and promote hydrogen-assisted

dehydrogenation of the CH_4 molecules, which in turn leads to the generation of C atoms required for graphene nucleation.[RS18,RS19] This effect becomes more effective when a Cu film (catalyst substrate) is evaporated and annealed in hydrogen gas (until the Cu substrate is heated to the growth temperature). This process leads to the formation of Cu(111) facets which (like Cu(110) facets)[RS20] are energetically most favorable sites for the adsorption of hydrogen atoms.[RS21] Therefore, graphene synthesis is possible through a hydrogen-free growth step due to dehydrogenation and possibly thermal decomposition of hydrocarbon molecules (hence, C production) by the hydrogen atoms pre-adsorbed during the annealing step.[RS18,RS19]

Main mobile C species on a Cu catalyst surface: a discussion.

Here we discuss the stability of mobile C monomers and dimers and their roles in the growth of monolayer graphene on a Cu catalyst surface. Since a very low energy is needed to overcome the energy barrier for C monomer diffusion on the Cu surface, the C monomers can easily diffuse on the surface and contribute to the formation of C clusters[RS22,RS23] and growth of larger graphene islands. Recently, Shu *et al.*[RS24] and Luo *et al.*,[RS25] using *ab initio* calculations, demonstrated that the growth of the initial graphene nuclei (and the formation of regularly shaped graphene islands) on a Cu catalyst surface is mostly determined by the incorporation of C monomers rather than C dimers. Strictly speaking, attachment of C monomers into the stable graphene-edge sites can be used as a viable mechanism to reasonably interpret the formation of large graphene islands with regular shapes observed in graphene growth experiments.[RS25]

However, a recent Density Functional Theory (DFT) calculation showed that a C monomer may be energetically unstable on a Cu catalyst surface.[RS26] This study also claimed that the formation of C dimers (and their diffusion and the subsequent formation of larger graphene islands) on the Cu catalyst surface is energetically favourable and the C dimers are more stable than the C monomers. In addition to this, first-principles calculations demonstrated

that generation of C monomers (and four hydrogen atoms) via direct thermal decomposition of methane (CH_4) molecules on a Cu surface is less favorable, which was interpreted as an instability of C monomers.[RS14] Therefore, stability of C monomers on the Cu surface is a highly debatable issue and more comprehensive investigations are warranted in order to better understand the most important C species (and their roles) in the growth of monolayer graphene on a Cu substrate commonly used in graphene synthesis.[RS25]

The role of 5-atom C clusters in graphene growth on a Cu surface: a discussion

Here we briefly discuss the important role of 5-atom C clusters in graphene growth on a Cu substrate surface. Relevant reports are extremely rare. However, recently Luo *et al.*[RS25] reported on the importance of 5-atom C cluster contribution to graphene growth on a Cu catalyst surface. Interestingly, attachment of 5-atom clusters to a zigzag-edged graphene island is the energetically favorable mechanism which provides stable binding sites for the attachment of the C monomers. [RS25] The calculations also showed that the rate of the cluster attachment (to the graphene edge) is lower than the rate of monomer attachment. Otherwise the growth of irregularly shaped graphene domains (on the Cu catalyst surface) is expected, which contradicts the experimental observations.[RS25,RS27] Therefore, 5-atom C clusters are crucial in the growth of monolayer graphene not only on the Ru/Ir catalyst layer, but also on the Cu catalyst layer.

Temperature dependence of graphene surface coverage: a brief report

Here we mention briefly the different trends of graphene coverage with variations in the substrate temperature and discuss the possible reasons for such the growth trends. As we mentioned in the main text, the graphene surface coverage increases with increasing in the catalyst temperature. This trend agrees with numerous graphene growth experiments.[RS16,RS28,RS29] This can be explained by the enhanced dehydrogenation of hydrocarbon molecules (thus generation of C atoms) at higher temperatures. In contrast,

the surface coverage is reduced upon further increasing the temperature which was observed in the experiments of graphene growth and C deposition by Vlassiouk *et al*.[RS5] and La Cava *et al.*,[RS16] respectively. Vlassiouk *et al*. expressed their observation as "we have verified that *the minimum temperature at which such etching (by hydrogen) noticeably occurs for graphene on Cu is no less than 850 °C*". Regarding this experimental evidence, it is clear that with increasing the temperature, while the hydrogen pressure is high, the graphene surface coverage should decrease. This is because not only the evaporation of C atoms (desorption of hydrocarbon precursor prior to undergoing dehydrogenation) becomes stronger, but also the rate of etching (by adsorbed hydrogen atoms, see reaction 11 in Table 1 of the main text) becomes stronger with increasing the substrate temperature. Apart from this, a recent experimental work by Olle *et al.*[RS30] reported a decrease of the total graphene surface coverage with further increasing the reaction temperature. In this work, more effective desorption of hydrocarbon molecules from the metal surface at high temperatures is mentioned as the most plausible reason for such an unusual behavior of the graphene surface coverage upon increasing the temperature.

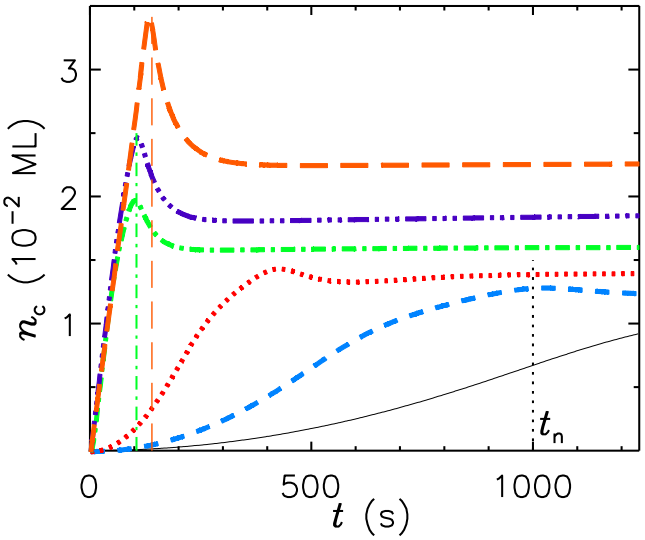

Figure S1. The evolution of C atom concentration at different temperatures. Solid, dashed, dotted, dash-dotted, dash-dot-dotted, and long-dashed curves correspond to $T = 550$, 570, 600, 700, 800, and 1020 K, respectively. Also, the hydrocarbon gas pressure is $P_{\mathrm{CH}} = 3\times10^{-6}$ mTorr.

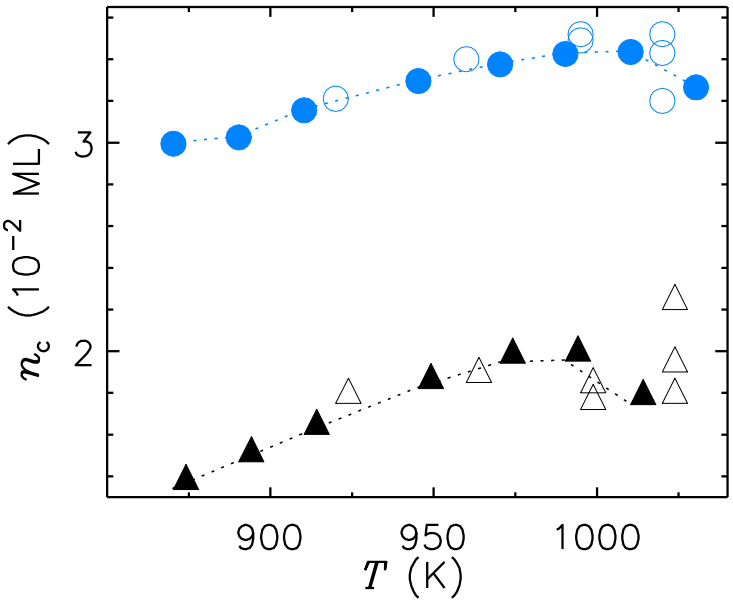

Figure S2. Comparison between results of the numerical modeling and LEEM measurement of graphene growth by exposing Ru catalyst surface to ethylene gas. The C atom concentrations in equilibrium with the graphene $n_{\mathrm{C}}^{\mathrm{eq}}$ (triangles) after the hydrocarbon flux is switched off and the C concentration required to nucleate graphene $n_{\mathrm{C}}^{\mathrm{nuc}}$ (circles) from solution of the rate equation (filled symbols) and the LEEM measurements (hollow symbols) of Loginova *et al.*[RS4] Also, the ethylene gas pressure is $P_{\mathrm{CH}} = 3\times10^{-6}$ mTorr .

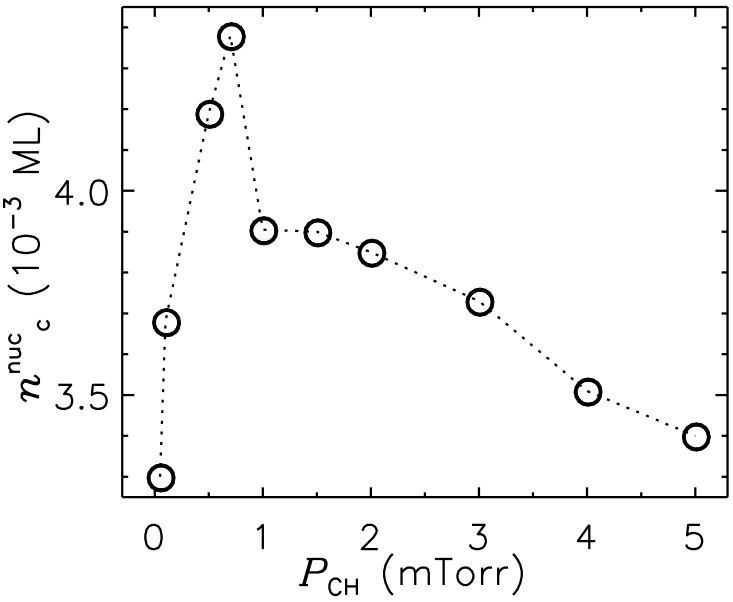

Figure S3. Effect of the hydrogen atoms on initiation of the graphene nucleation and etching of the BUs from Cu catalyst surface. The C atom concentrations required to nucleate graphene $n_{\mathrm{C}}^{\mathrm{nuc}}$ (circles) from the solution of a set of rate equations. Total gas pressure and catalyst temperature are $P = 10\ \mathrm{mTorr}$ and $T = 823\ \mathrm{K}$, respectively.

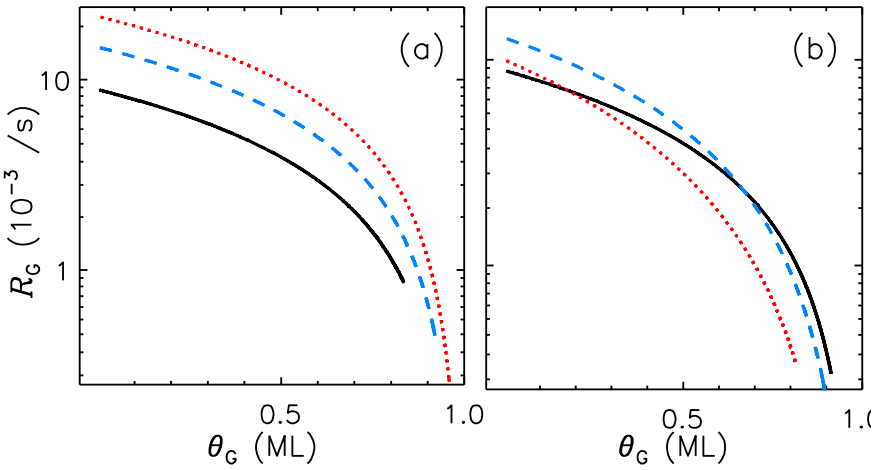

Figure S4. Effect of the process parameters on the graphene growth. The graphene growth rate R_G as a function of graphene coverage θ_G for three different hydrocarbon gas pressures (a) and Cu catalyst temperatures (b). Solid, dashed, and dotted curves in (a) correspond to $P_{CH} = 1$, 2, and 6 mTorr, respectively, while the same curves in (b) correspond to $T = 823$, $T = 873$, and 923 K, respectively. Unless varied in any particular plot, the default set of parameters is $T = 823$ K, $P = 10$ mTorr, $P_H = 1.25$ mTorr, and $P_{CH} = 1.0$ mTorr.

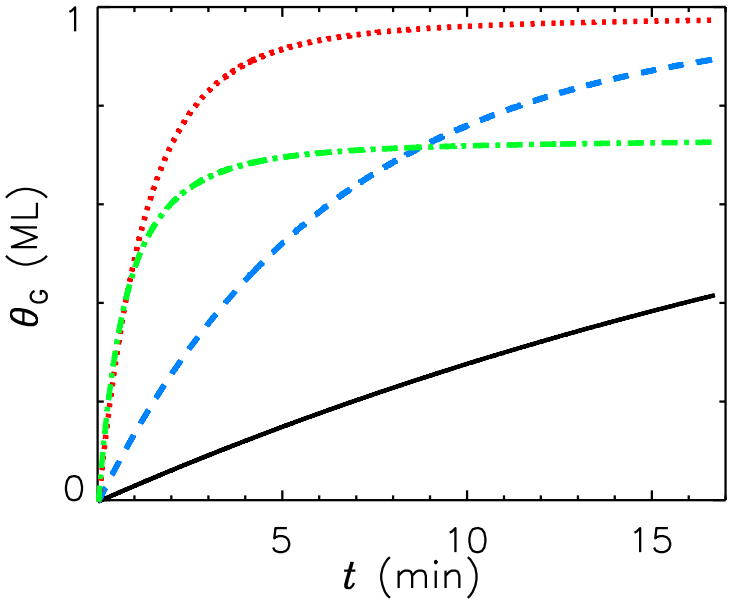

Figure S5. Effect of temperature on hydrogen etching of the graphene. The time evolutions of graphene surface coverage θ_G at four different Cu catalyst temperatures. Solid, dashed, dotted, and dashed-dotted curves correspond to $T = 573$, $T = 813$, $T = 873$, and $1023\ \mathrm{K}$, respectively. The default set of parameters is $P = 10\ \mathrm{mTorr}$, $P_H = 9.0\ \mathrm{mTorr}$, and $P_{CH} = 1.0\ \mathrm{mTorr}$.

References

RS1. Ostrikov, K.; Mehdipour, H. Thin Single-Walled Carbon Nanotubes with Narrow Chirality Distribution: Constructive Interplay of Plasma and Gibbs-Thomson Effects. *ACS Nano* **2011**, *5*, 8372-8382.

RS2. Lysaght, A. C.; Chiu, W. K. S. Modeling of the Carbon Nanotube Chemical Vapor Deposition Process Using Methane and Acetylene Precursor Gases. *Nanotechnology* **2008**, *19*, 165607.

RS3. Gao, L.; Guest, J. R.; Guisinger, N. P. Epitaxial Graphene on Cu(111). *Nano Lett.* **2010,** *10*, 3512–3516.

RS4. Loginova, E.; Bartelt, N. C.; Feibelman, P. J.; McCarty, K. F. Factors Influencing Graphene Growth on Metal Surfaces. *New Journal of Physics* **2009**, *11*, 063046.

RS5. Vlassiouk, I., Regmi, M.; Fulvio, P.; Dai, S.; Datskos, P.; Eres, G.; Smirnov, S. Role of Hydrogen in Chemical Vapor Deposition Growth of Large Single-Crystal Graphene. *ACSNano* **2011**, *5*, 6069–6076.

RS6. Loginova, E.; Bartelt, N. C.; Feibelman, P. J.; McCarty, K. F. Evidence for Graphene Growth by C Cluster Attachment. *New Journal of Physics* **2008**, 10**,** 093026.

RS7. Wang, B.; Ma, X.; Caffio, M.; Schaub, R.; Li, W. –X. Size-Selective Carbon Nanoclusters as Precursors to the Growth of Epitaxial Graphene. *Nano Lett.* **2011**, *11*, 424–430.

RS8. Yuan, Q.; Gao, J.; Shu, H.; Zhao, J.; Chen, X.; Ding, F. Magic Carbon Clusters in the Chemical Vapor Deposition Growth of Graphene. *J. Am. Chem. Soc.*, **2012**, *134*, 2970–2975.

RS9. Zangwill, A.; Vvedensky, D. D. Novel Growth Mechanism of Epitaxial Graphene on Metals. *Nano Lett.* **2011**, *11*, 2092–2095.

RS10. Gao, J.; Yip, J.; Zhao, J.; Yakobson, B. I.; Ding, F. Graphene Nucleation on Transition Metal Surface: Structure Transformation and Role of the Metal Step Edge. *J. Am. Chem. Soc.* **2011**, *133*, 5009–5015.

RS11. Stoldt, C. R.; Jenks, C. J.; Thiel, P. A.; Cadilhe, A. M.; Evans, J. W. Smoluchowski ripening of Ag islands on Ag(100). *J. Chem. Phys.* **1999**, *111*, 5157- 5166.

RS12. Li, Z.; Wu, P.; Wang, C.; Fan, X.; Zhang, W.; Zhai, X.; Zeng, C.; Li, Z.; Yang, J.; Hou, J. Low-Temperature Growth of Graphene by Chemical Vapor Deposition Using Solid and Liquid Carbon Sources. *ACSNano* **2011**, *5*, 3385–3390.

RS13. Li, X.; Magnuson, C. W.; Venugopal, A.; An, J.; Suk, J. W.; Han, B.; Borysiak, M.; Cai, W.; Velamakanni, A.; Zhu, Y.; Fu, L.; Vogel, E. M.; Voelkl, E.; Colombo, L.; Ruoff, R. S. Graphene Films with Large Domain Size by a Two-Step Chemical Vapor Deposition Process. *Nano Lett.* **2010**, *10*, 4328-4334.

RS14. Zhang, W.; Wu, P.; Li, Z.; Yang, J. First-Principles Thermodynamics of Graphene Growth on Cu Surfaces. *J. Phys. Chem. C* **2011**, *115*, 17782–17787.

RS15. Alstrup, I.; Chorkendorff, I.; Ullmann, S. The Interaction of CH_4 at high Temperatures with Clean and Oxygen Precovered Cu(100). *Surf. Sci.* **1992**, *264*, 95-102.

RS16. La Cava, A. I.; Bernardo, C. A.; Trimm, D. L. Studies of Deactivation of Metals by Carbon Deposition. *Carbon* **1982**, *20*, 219-223.

RS17. Grujicic, M.; Cao, G.; Gersten, B. Optimization of the Chemical Vapor Deposition

Process for Carbon Nanotubes Fabrication. *Appl. Surf. Scie.* **2002**, *19*,223-239.

RS18. Tao, L.; Lee, J.; Chou, H.; Holt, M.; Ruoff, R. S.; Akinwande, D. Synthesis of High Quality Monolayer Graphene at Reduced Temperature on Hydrogen-Enriched Evaporated Copper (111) Films. *ACS Nano* **2012**, *6*, 2319–2325.

RS19. Lee, S.; Lee, K.; Zhong, Z. Wafer Scale Homogeneous Bilayer Graphene Films by Chemical Vapor Deposition. *Nano Lett.* **2010,** *10*, 4702–4707.

RS20. Stromquist, J.; Bengtsson, L.; Persson, M.; Hammer, B. The Dynamics of H Absorption in and Adsorption on Cu(111). *Surf. Sci.* **1998**, *397*, 382–394.

RS21. Thomsen, L.; Onsgaard, J.; Godowski, P. J.; Møller, P.; Hoffmann, S. V. Adsorption of Hydrogen on Clean and Potassium Modified Low Index Copper Surfaces: Cu(100) and Cu(110). *J. Vac. Sci. Technol. A*, **2001**, *19*, 1988–1992.

RS22. Yazyev, O. V.; Pasquarello, A. Effect of Metal Element in Catalytic Growth of Carbon Nanotubes. *Phys. Rev. Lett.* **2008**, *100*, 156102.

RS23. Van Wesep, R. G.; Chen, H.; Zhu, W.; Zhang, Z. Communication: Stable Carbon Nanoarches in the Initial Stages of Epitaxial Growth of Graphene on Cu(111). J. Chem. Phys. **2011**, *134*, 171105.

RS24. Shu, H.; Chen, X.; Tao, X.; Ding, F. Edge Structural Stability and Kinetics of Graphene Chemical Vapor Deposition Growth. *ACS Nano*, **2012**, *6*, 3243–3250.

RS25. Luo, Z.; Kim, S.; Kawamoto, N.; Rappe, A. M.; Johnson, A. T. C. Growth Mechanism of Hexagonal-Shape Graphene Flakes with Zigzag Edges. *ACS Nano* **2011**, *11*, 9154-9160.

RS26. Riikonen, S.; Krasheninnikov, A. V.; Halonen, L.; Nieminen, R. M. The Role of Stable and Mobile Carbon Adspecies in Copper-Promoted Graphene Growth. *J. Phys. Chem. C.* **2012**, *116*, 5802-5809.

RS27. Yu, Q.; Jauregui, L. A.; Wu, W.; Colby, R.; Tian, J.; Su, Z.; Cao, H.; Liu, Z.; Pandey, D.; Wei, D. *et al.* Control and Characterization of Individual Grains and Grain Boundaries in Graphene Grown by Chemical Vapour Deposition. *Nature Mater.* **2011**, *10*, 443-449.

RS28. Kim, H.; Mattevi, C.; Calvo, M. R.; Oberg, J. C.; Artiglia, L.; Agnoli, S.; Hirjibehedin, C. F.; Chhowalla, M.; Saiz E. Activation Energy Paths for Graphene Nucleation and Growth on Cu. *ACS Nano*, **2012**, *6*, 3614–3623.

RS29. Li, X.; Magnuson, C. W.; Venugopal, A.; An, J.; Suk, J. W.; Han, B.; Borysiak, M.; Cai, W.; Velamakanni, A.; Zhu, Y. *et al.* Graphene Films with Large Domain Size by a Two-Step Chemical Vapor Deposition Process. *Nano Lett.* **2010**, *10*, 4328-4334.

RS30. Olle, M.; Ceballos, G.; Serrate, D.; Gambardella, P. Yield and Shape Selection of Graphene Nanoislands Grown on Ni(111). *Nano Lett.* **2012**, dx.doi.org/10.1021/nl300897m.